Volume 300, number 1, 49–55 FEBS 10862 March 1992

Structure and RNA content of the prosomes*

Olivier Coux[a], Hans G. Nothwang[a], Klaus Scherrer[a], Wilma Bergsma-Schutter[b], Annika C. Arnberg[b], Peter A. Timmins[c], Jörg Langowski[d] and Claudine Cohen-Addad[c,e]

[a]*Institut Jacques Monod, 2 place Jussieu, Tour 43, 75251 Paris Cedex 05, France,* [b]*Bioson Research Institute, Department of Chemistry, University of Groningen, Nijenborgh 4, 9747 AG Groningen, The Netherlands,* [c]*Institut Laue-Langevin, B.P. 156 X, 38042 Grenoble Cedex, France,* [d]*E.M.B.L. Outstation, c/o ILL, B.P. 156 X, 38042 Grenoble Cedex, France* and [e]*Laboratoire de Biologie Structurale, CNRS, URA 1333, Centre d'Etudes Nucléaires, BP 85 X, 38041 Grenoble Cedex, France*

Received 7 January 1992; revised version received 12 February 1992

Duck erythroblasts prosomes were analysed by small angle neutron scattering (SANS), dynamic light scattering and cryo-electron microscopy. A molecular weight of ~ 720,000 ± 50,000, a radius of gyration of 64 ± 2 Å and a hydrodynamic radius of ~ 86 Å were obtained. Electron micrographs show a hollow cylinder-like particle with a diameter of 120 Å, a height of 170 Å and a diameter of 40 Å for the cavity, built of four discs, the two outer ones being more pronounced than those in the center. Results from SANS indicate less then 5% of RNA in the purified prosomes, but nuclease protection assays confirm its presence.

Prosome; Multicatalytic proteinase; Proteasome; Neutron scattering; Light scattering; Electron microscopy

1. INTRODUCTION

Prosomes, a class of small cytoplasmic RNP complexes first observed in HeLa cells [5] were characterized in duck and mouse erythroblasts as a subcomplex of repressed mRNPs [1,6]. As found later, these particles are identical to the multicatalytic protease complex (MCP), characterized by others [4,7]. The particles are ubiquitous from archaebacteria to the human species and are localized in eukaryotic cells both in the nucleus and the cytoplasm (for review, see [8,9]). In the latter, they are associated with the Intermediate Filaments of the cytoskeleton [10]. Their most outstanding physical property is their high molecular weight. The individual particle is a multisubunit complex consisting of a variable set of 15–30 polypeptides with molecular masses of 19–36 kDa [6,11–13]. Although the presence of a small RNA with a length of 80–120 nucleotides is well documented for prosomes [1,6,7,14], controversy still exists over its quantity. The original (over-) estimation of 15% was based on a density of 1.31 g/cm^3 and Spirin's formula of RNA content versus density of RNP complexes [15].

The cellular function(s) of prosomes remains, however, speculative. Several specific properties and enzymatic activities have been claimed to be associated with prosomes (for review see [8,9]). Among them, their multicatalytic proteinase activity is actually the best characterized. Recently it was also shown that prosomes are a constituent part of a 26S proteolytic complex, involved in the ATP dependent selective ubiquitin-conjugated protein breakdown [16,17].

Since the size and shape of the particles as well as some of their protein subunits show a very high conservation in evolution [6,18], the morphological structure of the complex seems to be of importance, and its elucidation might offer a potential key for a better understanding of the function(s) of prosomes. Although a large body of data concerning the physical and chemical characteristics of the particle accumulated in the last years there is still disagreement on the precise dimensions and its shape [5,6,18–22]. Therefore to obtain additional information on the structural features, and to compare data based on different methods we examined the size, shape and other physical characteristics as well as the genuine RNP character of this particle by EM, dynamic light scattering, and small angle neutron scattering. The latter method was also chosen, as it allows to distinguish, in contrast to small angle X-ray scattering for example, between nucleic acids and proteins; therefore it might be a tool to determine the relative position of the RNA and protein moities and, in addition, some estimation of the RNA content of prosomes.

*We use here the term 'Prosome' introduced by our laboratory (Schmid et al., 1984) for the then unknown particle and, speaking of its protease activity, the term 'Multicatalytic Proteinase or MCP' according to the recommendation of the group of enzymologists (Dahlman et al., 1988; and Orlowski and Wilk, 1988), in preference to the term 'Proteasome' suggested by Arrigo et al. (1988) [1–4].

Correspondence address: K. Scherrer, Institut Jacques Monod, 2 place Jussieu, F-75251 Paris Cedex 05, France. Fax: (33) (1) 46332305.

2. MATERIALS AND METHODS

2.1. *Isolation and purification of prosomes*

The isolation and purification of duck erythoblasts, the subsequent preparation of the post-ribosomal supernatant by cell fractionation and the purification of the untranslated 20S globin-free mRNPs were as described [23,24]. The isolation and purification of the prosomes from these mRNPs by sucrose gradients in the presence of 0.5 M KCl or 0.1% sarkosyl has been reported [1]. For RNA-protection and -quantification assays, prosomes were additionally subjected to a final purification step consisting in a gel filtration using a FPLC Superose 6 column (Pharmacia-LKB). Protein concentration of the purified particle preparation was determined by the method of Bradford [25] using BSA as a standard.

2.2. *Nuclease digestion assay*

The samples (10 μg prosomes), either dissociated or not by Zn^{2+} were exposed in a final volume of 50 μl to ribonuclease V1 digestion in a buffer containing 0,02 M TEA-HCl (pH 7.4), 0.2 M NaCl, 10 mM $MgCl_2$ at 37°C. The reaction was stopped by adding 200 μl phenol. The RNA was labeled after phenol extraction at the 3' end with [^{32}P]pCp in a reaction catalyzed by T4 RNA ligase [26]. The RNA fragments were analysed by 10% acrylamide/8 M urea gel electrophoresis followed by autoradiography.

2.3. *Small angle neutron scattering (SANS)*

Samples for neutron scattering were prepared from a stock solution of prosomes at 1.3 mg/ml in a buffer containing 10% (w/v) glycerol, 10mM Tris-HCl (pH 7.4), 50 mM KCl and 5 mM β-mercaptoethanol in either H_2O or D_2O. Solutions containing various proportions of D_2O/H_2O were then prepared by mixing the D_2O and H_2O prosome solutions. Buffer solutions of the same isotopic composition were prepared in the same manner. Solutions were thus prepared in which the water contained 0, 15, 55, 70, 85 and 100% D_2O corresponding to volume fractions of 0.9 times the value of the total solution (the other 10% was glycerol). D_2O contents of sample and buffer were verified by neutron transmission measurements (see below).

SANS measurements were carried out on the small angle scattering instrument D11 [27] at the High Flux Reactor of the Institut Laue-Langevin, Grenoble. Samples, prepared as above, were put into quartz cuvettes (Hellma, France) of 1- or 2-mm pathlength presenting a cross-sectional area of ~70 mm^2 to the incident neutron beam. Experiments were carried out using neutrons of wavelength (λ) 10 Å with a wavelength spread ($\Delta\lambda/\lambda$) of 0.09 (FWHM). The two-dimensional multi-detector (64 × 64 cm) was placed at 10 meters from the sample allowing scattering to be recorded in the momentum transfer range $3 \times 10^{-3} < Q < 2.3 \times 10^{-2}$ Å^{-1} ($Q = 4\pi\sin\theta/\lambda$, 2θ=scattering angle). Data collection times varied from 0.5 h for samples in 100% D_2O to ~3 h for samples at low contrast (55% D_2O). The data were circularly averaged about the origin of the diffraction pattern, and corrected for buffer scattering and detector response using a standard suite of programs [28]. This process yielded a curve of scattered intensity as a function of momentum transfer, $I(Q)$ vs. Q, for each D_2O buffer and hence each contrast.

Curves were plotted as Guinier plots (ln$I(Q)$ vs. Q^2) from which two model-independent parameters may be derived, i.e. the radius of gyration (R_g) and the intensity at zero angle ($I(0)$) [29].

2.4. *Dynamic light scattering (DLS)*

Dynamic light scattering was used to determine the hydrodynamic radius R_h of the prosome particles under various H_2O/D_2O ratios and glycerol contents. The apparatus used for the DLS experiments consisted of a BI 2030 AT 4°N-bit autocorrelator with 128 real-time channels (Brookhaven Instruments, Ronkonkoma, USA), a stepping-motor goniometer (Amtec, Nice), and a Spectra-Physics 2025 5W argon ion laser. The laser was running at a power of 500 mW on the 488 nm line. The sample was contained in a 1-cm diameter cylindrical quartz cuvette immersed in an 8-cm diameter index matching bath filled with 0.2 μm-filtered distilled water. The sample was introduced into the cuvette through a 0.1 μm nucleopore polycarbonate membrane filter, through which the cuvette had also been rinsed before with sample buffer. All measurements were done with the measuring cell thermostated to (20 ± 0.2)°C.

A total of 7 samples were measured: one each with the sample in pure H_2O and H_2O + 10% glycerol, three samples in pure D_2O, and two in D_2O + 10% glycerol, one of which had been centrifuged in a Beckman airfuge at 180,000×g for 15 min to remove eventual aggregates.

In each DLS run, autocorrelation functions $G^2(\tau)$ were collected at 15 different scattering angles between 25° and 140°. The data were then analyzed simultaneously for all scattering angles using a three-component model. Each independently diffusing component in the solution contributes to an independent exponential decay in a squared sum of exponentials:

$$G^2(\tau) = 1 + [a_1(k)e^{-k^2D_1\tau} + a_2(k)e^{-k^2D_2\tau} + a_3(k)e^{-k^2D_3\tau}]^2 \qquad (1)$$

The three components of $G^2(\tau)$ correspond to the diffusion of the principal component a_1, to photomultiplier afterpulsing and diffusion of small components such as the glycerol a_2, and diffusion of larger aggregates and minor dust contaminations a_3, respectively. D_1, D_2 and D_3 are their diffusion coefficients, which are assumed to be independent of the scattering vector K, while the amplitudes are allowed to vary with K. K is defined as

$$K = \frac{4\pi n}{\lambda}\sin\left(\frac{\theta}{2}\right) \qquad (2)$$

where λ is the wavelength of the scattered light, n the refractive index of the solution and θ the scattering angle.

2.5. *Electron microscopy*

A stock solution of purified prosomes, containing 1.4 mg/ml protein in 10 mM TEA-HCl (pH 7.4), 50 mM KCl and 5% β-mercaptoethanol was diluted 10 times in 50 mM ammonium acetate. Aliquots of 5 μl were applied to positively charged formvar-carbon coated grids and stained with 2% (w/v) sodium phosphotungstate (pH 7.5). Specimens were analyzed in a JEOL 1200EX or a Philips CM12 microscope.

Cryo-electron microscopy was essentially as described by Adrian et al., (1984) and Dubochet et al., (1988) [30,31]. Aliquots of prosomes (0.3 mg/ml in 50 mM ammonium acetate) were applied to perforated carbon films. Most of the solution was removed by pressing a piece of filter paper directly against the entire grid surface before rapid plunging into liquid ethane, cooled by liquid nitrogen, using a KF80 cryo-unit from Reichert. Specimens were transferred to liquid ni-

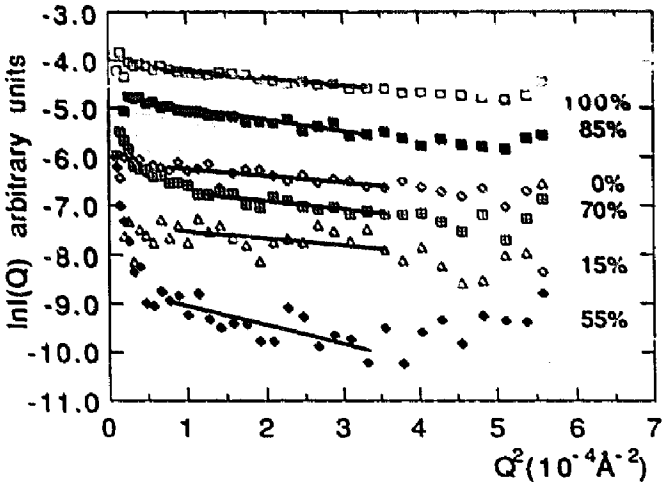

Fig. 1. Small angle neutron scattering curves plotted as Guinier plots, ln $I(Q)$ vs. Q^2. The D_2O percentage in the buffer is shown against each curve. The ordinate values, however, have been arbitrarily shifted for ease of viewing.

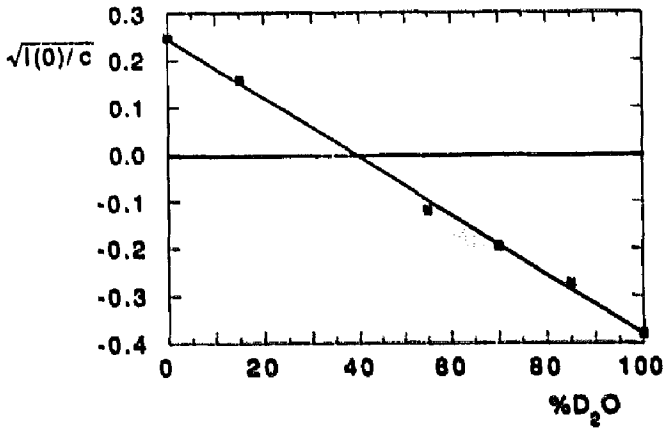

Fig. 2. Plot of $\sqrt{I(0)/c}$ vs. buffer D_2O content. The $I(0)$ values, obtained from the scattering curves shown in Fig. 1, have been normalized to unit concentration, thickness and transmission.

trogen and introduced into a cryo-specimen holder (Gatan Inc. Warrendale, PA type 626) and analyzed in a JEOL 1200 EX microscope equipped with a Gatan anticontaminator. Specimens were observed at temperatures of about −175°C and at 80 kV. Micrographs of the frozen-hydrated samples were recorded at nominal magnifications of 50,000× or 60,000× on Kodak SO-163 film at an underfocus of 2.4 μm. Exposed micrographs were developed for 12 min in full-strength D-19 developer.

3. RESULTS

3.1. *Small angle neutron scattering*

The scattering curves obtained at 6 different D_2O contents are shown in Fig. 1 displayed as Guinier plots. The quality of these plots is rather poor and strongly limits the amount of information we can derive from the data. The limitations are due mainly to very poor signal-to-noise ratio in the lowest contrasts (15 and 55% D_2O), and to the presence of high molecular weight aggregates in some samples. The former problem cannot be resolved without a very significant increase in sample concentration which at present is not possible. The data in 0% and 100% D_2O are, however, of good quality, and the following analysis is based primarily on these two curves.

Fig. 2 shows $\sqrt{I(0)/c}$ (c = concentration) as a function of D_2O buffer content. The point at which the fitted straight line crosses the abscissa indicates the buffer composition at which the particle has zero contrast, the so-called contrast match point, and is dependent on the chemical composition of the scattering particle. The observed match point is at a buffer composition of 39.2% D_2O corresponding to a solvent scattering length density of 2.046×10^{-14} cm·Å^{-3}. Assuming that the glycerol is distributed homogeneously throughout the solvent and is not preferentially adsorbed to or excluded from the molecular surface, this is equivalent to a match-point of ~37.4% D_2O in a pure water mixture. As the contrast match-point of soluble proteins usually lies within the range of 40–43% D_2O and that of RNA close to 69% D_2O we therefore conclude that the prosome particles contain little if any RNA, certainly less than 15% and possibly less then 5% or one RNA molecule per particle.

From the value of $I(0)$ obtained for the particle in 0% D_2O (where the data quality is good) we can estimate the molecular weight of the particle [32]. For this we require the concentration of the sample and a knowledge of the RNA/protein stoichiometry. The concentration was determined by the method of Bradford using BSA as the standard; a value of 1.3 mg/ml was obtained. The particle stoichiometry is in principle derivable from the plot of $\sqrt{I(0)/c}$ vs. D_2O content, although, in our case this is rather imprecise, as explained above. We can however place limits on the stoichiometry and calculate that the molecular weight is between 686,000 ± 50,000 and 671,000 ± 50,000 corresponding to an RNA content of 0% and 5%, respectively. The estimated error of 50,000 in the molecular weight determination stems from the statistical error of the $I(0)$ measurement only and assumes that errors in the concentration measurement are less than 5%.

The radius of gyration obtained from the Guinier plots are 64 ± 7Å in 0% D_2O and 64 ± 2Å in 100% D_2O. This value is rather large compared with that expected for a compact particle of a similar molecular weight. It is, for example, very close to that measured for the icosahedral enzyme complex heavy riboflavin synthase [33] which has a molecular weight of 1.0^6. We therefore conclude from the SANS result that the prosome must be an elongated particle or have its subunits rather loosely packed.

It is not possible to derive any information about the

Table I

Comparison of EM, SANS and DLS measurements on prosome particles

Method	Dimensions	R_g (calc)	R_g (obs)	R_H (calc)	R_H (obs)	M
TEM	120 × 170 (Å)	64.9 (Å)	–	81 (Å)	–	–
Cryo-TEM	110 × 160 (Å)	–	–	–	–	720,000
SANS	–	–	64 ± 2 (Å)	–	–	[a]680,000±50,000 [b]671,900±50,000
DLS	–	–	–	–	86±7 (Å)	763,000±62,000

[a]Estimated with 0% RNA, [b]Estimated with 5% RNA.

relative location of any RNA associated with the particle due to the large errors in the radii of gyration at intermediate D_2O contents.

3.2. *Dynamic light scattering*

The measurements from the seven samples, after correction for D_2O and glycerol viscosity using values from standard tables (CRC Handbook of Chemistry and Physics, 56th edn.), gave the same value for the diffusion coefficient of the prosome particle, $D = (2.5 \pm 0.2) \cdot 10^{-11}$ [$m^2 \cdot s^{-1}$]. This corresponds to a hydrodynamic radius R_h: 86 ± 7 Å. The relative amplitude of the component of the scattered light from larger aggregates was approx. 25–40% depending on the scattering angle, with larger values at low scattering angles. No significant change could be seen in the sample which had been centrifuged in the Airfuge. The aggregates are characterized by a hydrodynamic radius which is at least 10 times larger than that of a main particle; for spherical particles this would correspond to a molecular weight — thus a relative scattering power — 10^3 times higher. This is an upper estimate, since we do not know the shape of eventual aggregates; even so, the weight proportion of large aggregates must be below 1% of the total sample.

The molecular weight of the particles can also be estimated: from the sedimentation coefficient $s = 19S$ [1] and the measured diffusion coefficient, and assuming a partial specific volume of 0.76 $cm^3 \cdot g^{-1}$, a molecular weight of M = 763,000 ± 62,000 is obtained, at the upper limit of Ms obtained by other techniques (see Table 1).

3.3. *Electron microscopy*

Negatively stained prosomes show a typical staining behaviour depending on the type of stain used. Uranyl acetate staining results in almost 100% ring-like profiles with a heavily stained central region, and outer diameters ranging from 110 Å to 150 Å. Other negative stains, such as ammonium molybdate, sodium phosphotungstate and sodium silicotungstate result in 70%, 60% and 30% ring-like profiles, respectively. The other profiles observed in these specimens are rectangular. An example of prosomes stained with sodium phosphotungstate is shown in Fig. 3. A mixture of ring-like and rectangular profiles observed in a specimen prepared from a monodisperse protein complex solution is characteristic for a cylinder-like structure. A projection along the long axis reveals a ring-like profile with a stained central region. In less than 2% (but up to 50% in 'aged' or EDTA treated preparations) of the ring-like profiles the central cavity is not visible; these profiles probably represent damaged particles. The central heavily stained region indicates that the cylinder-like particle is hollow. Rectangular profiles represent cylinder-like molecules laying on their side on the support film. From measurements of the diameter of ring-like profiles and the length of rectangular profiles it was found that the particles correspond to a cylinder-like molecule with a diameter of 120 Å and a height of 170 Å. The central hole varies in size and shape, especially in uranyl acetate-stained specimens, but we estimated the diameter of the hole to be about 40 Å.

In the ring-like profiles little or no substructure can be observed. However, the rectangular profiles are in accordance with a structure being build up of four discs. These discs are not identical because the two outer ones are more pronounced than the two central ones in the images.

Prosome particles were also prepared in the frozen hydrated state and visualized with cryo-electron microscopy (Fig. 4). With this method, bio-macromolecules can be analyzed in an unstained and hydrated state. Prosomes were imaged over holes in a perforated carbon film thereby avoiding eventual flattening or deformation of the particles due to adsorption to a support film. Ring-like and rectangular profiles were observed which strongly suggests that the prosomes

Fig. 3. Electron micrograph of prosomes, negatively stained with sodium phosphotungstate, showing ring-like profiles with a stained central region and rectangular profiles. Bar represents 500 Å;.

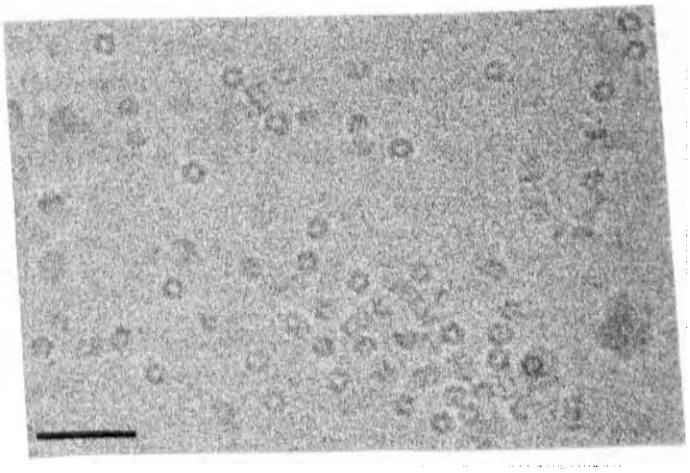

Fig. 4. Cryo-electron micrograph of unstained, hydrated prosome particles. The micrograph has recorded at 2.4 μm under focus. Bar represents 500 Å;.

exist as cylinder-like molecules in solution. The frozen hydrated prosomes had a diameter of 110 Å and a height of about 160 Å and a central cavity of about 40 Å. We calculated the volume of these particles assuming that the central hole observed in the ring-like profiles represents a water-filled channel through the particle. Based on the calculated volume and a hydration of 30% for the protein, we find that the prosomes particles have a molecular weight of approximately 720 kDa.

3.4. *Nuclease protection assay*

Small angle neutron scattering studies indicated only a low content of prosomal RNA in the particle, a result which was confirmed by optical density measurements (not shown). This raised the question whether or not the RNA found in the particle was due to a contamination in the preparation of prosomes from duck erythroblasts. To check this hypothesis, prosomes purified by ultracentrifugation in 0.5 M KCl sucrose gradients, followed by 0.1% Sarkosyl sucrose gradients were submitted to a further purification step by gel filtration on FPLC Superose 6 columns (Pharmacia). An aliquot of these prosomes were then phenol-extracted and analysed for the RNA content in the aqueous phase by 3'-end labeling. As shown in Fig. 5, an RNA about 80 nucleotides in length still purified with prosomes.

To prove unambiguously that this RNA is an intrinsic part of the prosomes from duck erythroblasts, we resorted to a stronger criterion. Recently we had observed that prosomes from both HeLa cells and duck erythroblasts can be dissociated in the presence of as little as 10^{-5} M Zn^{2+} without alteration of its constituent protein and RNA subunits, and that this dissociation is conditional for nuclease digestion of the RNA of HeLa cell prosomes (Nothwang et al., submitted). To prove that the same is also true for the prosomes from duck erythroblasts, studied by SANS, DLS and EM, aliquots of purified prosomes were incubated in the presence or absence of excess Zn^{2+} (10^{-3} M), prior to nuclease digestion. Breakdown of the particles in the presence of Zn^{2+} was monitored by the loss of their proteinase activity. As seen in Fig. 5, intact prosome particles apparently protected the full length of their RNA, whereas after disruption of prosomes, the RNA was readily digested by the V1 nuclease.

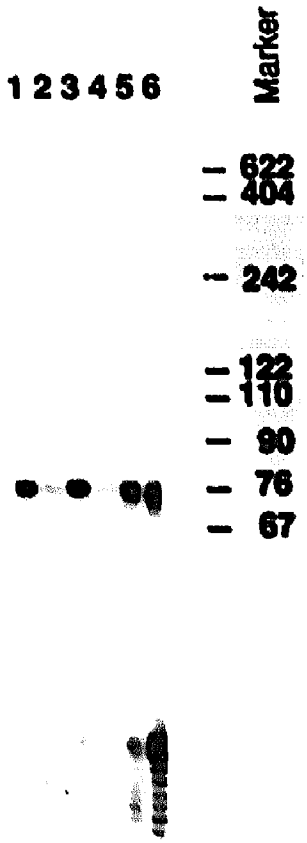

Fig. 5. Polyacrylamide/urea gel electrophoresis of pRNA after nuclease protection assay in presence or absence of Zn^{2+}. 10 μg of purified prosomes were incubated at 37°C in the absence or presence of 1 mM Zn^{2+} in a final volume of 20 μl. After 1 h, 1 mM EDTA was added prior to nuclease digestion by the V1 nuclease. After the reaction, the samples were phenol extracted, the RNA subsequently 3' end labeled, separated on a 10% polyacrylamide/8 M Urea gel, and visualized by autoradiography (12h). Lanes (1) and (3), prosomes incubated in the absence of Zn^{2+} prior to ribonuclease digestion with 25 U/ml V1 for 20 or 40 min, respectively; lanes (2) and (4), prosomes incubated in the presence of 1 mM Zn^{2+} prior to ribonuclease digestion with 25 U/ml V1 nuclease for 20 or 40 min, respectively; lanes (5) and (6), prosomes incubated in the absence or presence of 1 mM Zn^{2+}, respectively, without ribonuclease digestion.

4. DISCUSSION AND CONCLUSION

A comparison of the various parameters derived for the prosome particle from the three techniques used is given in Table I. Electron microscopy of the negatively stained prosome particles reveal ring-like and rectangular profiles, the relative proportions of each depending on the conditions of staining used. Measurements of these profiles suggest a cylindrical particle with a height of 170 Å and a diameter of 120 Å having an axial hole of ≤ 40 Å in diameter. Assuming the solvent contained in this cylindrical bore is dragged with the particle upon diffusion, we can approximate the hydrodynamic radius of the prosome as seen in EM by that of a solid cylinder of these dimensions. The friction factor of such a cylinder of an axial ratio close to 1 is practically identical to that of a sphere of equal volume [34]. This means that the particle as seen as in the EM would have a hydrodynamic radius of R_h = 81 Å. Within experimental error, this value is equal to that found by DLS. The corresponding radius of gyration of such a rod-like particle is given by:

$$R_g^2 = \frac{a^2}{3} + \frac{b^2}{2}$$

where a is the half length and b the radius. This leads to a value R_g = 64.9 Å which is in good agreement with the SANS measurements.

It would therefore appear that the particle in solution has a shape rather close to that observed in negative stain. This is also confirmed by the electron microscope images of frozen hydrated particles which are some 5–7% smaller in linear dimensions.

The molecular weight suggested by averaging all three techniques is ~ 720,000 ± 50,000, quite similar to that found for the large multicatalytic proteinase complex from rat skeletal muscle [19,20], but somewhat higher than the 600 kDa found previously [35].

The shape and dimensions found are remarkably similar to those reported for a number of 19S cylinder-like particles isolated from various eucaryotic cells [6,11,19]. Furthermore, a 19S particle with similar function and almost identical size and shape as the eucaryotic particles has been isolated from an archaebacterium [21,36].

Although several groups have clearly established during the last few years the presence of RNA in the particle [1,6,7,14], the stoichiometric relationship between RNA and protein is still a matter of controversy. Early data by Schmid et al. suggested for cytoplasmic prosomes an RNA content up to 15% [1], based on the formula of Spirin correlating RNA/protein content in RNP complexes [15]. Kleinschmidt and collegues, working with nuclear particles from oocytes, calculated from the absorbance ratio less than 0.1 RNA molecules per particle [37]. Our experiments presented here do not allow any precise positioning in the particle nor quantification of this RNA. This was in part due to their low amount, which is certainly less than 15% and probably less then 5% or one RNA per particle, and due to the large uncertainty in the radii of gyration in the analysis.

Thus, we can not conclude whether all prosomes or only a subpopulation of them contain RNA. It has to be taken into account that at least part of the RNA might be lost during extensive purification procedures like differential ultracentrifugation, using high ionic strength or especially by isolation methods which make use of several chromatographic steps. Indeed, data presented by Rivett and co-workers and our own group revealed, that using immunoprecipitation as a fast and gentle purification procedure, a higher amount and a more heterogenous population of pRNA was detected compared to isolation by alternative methods [14] (and Nothwang et al., submitted).

However, the nuclease digestion assay in the presence or absence of Zn^{2+}, as shown here for prosomes of duck erythroblasts and previously for prosomes from HeLa cells (Nothwang et al., submitted), seems clearly to demonstrate that the RNA found to copurify with prosomes is an intrinsic part of at least a fraction of these particles. However, the precise function(s) of the prosomes and their RNA, possibly in protein synthesis and metabolism, needs further elucidation.

Acknowledgements: We are grateful to R. Schwartzmann for help in the preparation of the manuscript and to M. Huesca for excellent technical assistance. O. Coux held a fellowship from the French Ministère de la Recherche et de la Technologie, and from the Association pour la Recherche sur le Cancer. H.G. Nothwang was supported by a fellowship from the Studienstiftung des Deutschen Volkes. This research was supported by grants to K.S. from the Centre National de la Recherche Scientifique, the Institut National de la Santé et de la Recherche Médicale, the Ligue Française contre le Cancer, the Fondation pour la Recherche Médicale Française, and the Association pour la recherche contre le Cancer (ARC), by Pro-Soma SARL and in part by the Netherlands Foundation of Chemical Research (SON), with financial support from the Netherlands Organization for Scientific Research (NWO).

REFERENCES

[1] Schmid, H.P., Akhayat, O., Martins de Sa, C., Puvion, F., Koehler, K. and Scherrer, K. (1984) EMBO J. 3, 29–34.
[2] Dahlmann, B., Kuehn, L., Ishiura, S., Tsukahara, T., Sugita, H., Rivett, J., Hough, R.F., Rechsteiner, M., Mykles, D.L., Fagan, J.M., Waxman, L., Ishii, S., Sasaki, M., Kloetzel, P.M., Harris, H., Ray, K., Behal, F.J., DeMartiono, G.N. and McGuire, M.J. (1988) Biochem. J. 255, 750.
[3] Orlowski, M. and Wilk, S. (1988) Biochem. J. 255, 751.
[4] Arrigo, A.P., Tanaka, K., Goldberg, A.L. and Welch, W.J. (1988) Nature 331, 192–194.
[5] Spohr, G., Granboulan, N., Morel, C. and Scherrer, K. (1970) Eur. J. Biochem. 17, 296–318.
[6] Martins de Sa, C., Grossi de Sa, M.F., Akhayat, O., Broders, F., Scherrer, K., Horsch, A. and Schmid, H.P. (1986) J. Mol. Biol. 187, 479–493.
[7] Falkenburg, P.E., Haass, C., Kloetzel, P.M., Niedel, B., Kopp, F., Kuehn, L. and Dahlmann, B. (1988) Nature 331, 190–192.
[8] Scherrer, K. (1990) Mol. Biol. Rep. 14, 1–9.
[9] Orlowski, M. (1990) Biochemistry 29, 10289–10297.
[10] Grossi de Sa, M.F., Martins de Sa, C., Harper, F., Olink-Coux, M., Huesca, M. and Scherrer, K. (1988) J. Cell Biol. 107, 1517–1530.
[11] Tanaka, K., Yoshimura, T., Ichihara, A., Ikai, A., Nishigai, M., Morimoto, Y., Sato, M., Tanaka, N., Katsube, Y., Kameyama, K. and Takagi, T. (1988) J. Mol. Biol. 203, 985–996.
[12] Pal, J.K., Gounon, P., Grossi de SA, M.F. and Scherrer, K. (1988) J. Cell Sci. 90, 555–567.
[13] Ahn, J.Y., Hong, S.O., Kwak, K.B., Kang, S.S., Tanaka, K., Ichihara, A., Ha, D.B. and Chung, C.H. (1991) J. Biol. Chem. 266, 15746–15749.
[14] Skilton, H.E., Eperon, I.C. and Rivett, A.J. (1991) FEBS Lett. 279, 351–355.
[15] Spirin, A.S., Belitsina, N.V. and Lerman, M.I. (1965) J. Mol. Biol. 14, 611–615.
[16] Eytan, E., Ganoth, D., Armon, T. and Hershko, A. (1989) Proc. Natl. Acad. Sci. USA 86, 7751–7755.
[17] Driscoll, J. and Goldberg, A.L. (1990) J. Biol.Chem. 265, 4789–4792.
[18] Tanaka, K., Yoshimura, T., Kumatori, A., Ichihara, A., Ikai, A., Nishigai, M., Kameyama, K. and Takagi, T. (1988) J. Biol. Chem. 263, 16209–16217.
[19] Kopp, F., Steiner, R., Dahlmann, B., Kuehn, L. and Reinauer, H. (1986) Biochim. Biophys. Acta 872, 253–260.
[20] Baumeister, W., Dahlmann, B., Hegerl, R., Kopp, F., Kuehn, L. and Pfeifer, G. (1988) FEBS Lett. 241, 239–245.
[21] Dahlmann, B., Kopp, F., Kuehn, L., Niedel, B., Pfeifer, G., Hegerl, R. and Baumeister, W. (1989) FEBS Lett. 251, 125–131.
[22] Hegerl, R., Pfeifer, G., Pühler, G., Dahlmann, B. and Baumeister, W. (1991) FEBS Lett. 283, 117–121.
[23] Vincent, A., Civelli, O., Maundrell, K. and Scherrer, K. (1980) Eur. J. Biochem. 112, 617–633.

[24] Gander, E.S., Stewart, A.G., Morel, C.M. and Scherrer, K. (1973) Eur. J. Biochem. 38, 443–452.
[25] Bradford, M.M. (1976) Anal. Biochem. 72, 248–254.
[26] England, T.E., Bruce , A.G. and Uhlenbeck, O.C. (1980) Methods Enzymol. 65, 65–74.
[27] Ibel, K. (1976) J. Appl. Cryst. 9, 296–309.
[28] Ghosh, R.E. (1989) internal Report 89 GHOZT, Institut Laue-Langevin, Grenoble.
[29] Guinier, A. and Fournet, G. (1955) Small Angle Scattering of X Rays, Wiley, New York.
[30] Adrian, M., Dubochet, J., Lepault, J. and Mc Dowell, A.W. (1984) Nature 308, 32–36.
[31] Dubochet, J., Adrian, M., Chang, J., J., H., Lepault, J., Mc Dowell, A.W. and Schultz, P. (1988) Q. Rev. Biopys. 21, 129–228.
[32] Jacrot, B. and Zaccai, G. (1981) Biopoloymers 20, 2413–2426.
[33] Ludenstein, R., Meyer, B., Huber, R., Labischinski, H., Bartels, K., Bartunik, H., Bachmann, L., Ludwig, H.C. and A., B. (1986) J. Mol. Biol. 187, 87–100.
[34] Tanford, C. (1961) Physical Chemistry of Macromolecules, Wiley, New York.
[35] Harris, J.R. (1988) Ind. J. Biochem. Biophys. 25, 459–466.
[36] Zwickl, P., Pfeifer, G., Lottspeich, F., Kopp, F., Dahlmann, B. and Baumeister, W. (1990) J. Struct. Biol. 103, 197–203.
[37] Kleinschmidt, J.A., Escher, C. and Wolf, D.H. (1988) FEBS Lett. 239, 35–40.